ELSEVIER

Journal of Photochemistry and Photobiology A: Chemistry 138 (2001) 95–109

Journal of Photochemistry and Photobiology A:Chemistry

www.elsevier.nl/locate/jphotochem

Transient absorption spectra of bifunctional probes of a chromophore-sterically hindered amine type in solution; study of the triplet route to deactivation

Pavol Hrdlovič [a,*], Štefan Chmela [a], Mohamed Sarakha [b], Jacques Lacoste [b]

[a] *Polymer Institute, Slovak Academy of Sciences, SK-84236 Bratislava, Dúbravská cesta 9, Slovak Republic*

[b] *Laboratoire de photochimie moleculaire et macromoleculaire, UMR CNRS 6505, Université Blaise Pascal, F-63177 Aubière Cedex, France*

Received 19 May 2000; received in revised form 21 August 2000; accepted 22 August 2000

Abstract

Laser flash photolysis was used to study formation and decay of triplet states of bifunctional probes of type chromophore (naphthalene, 1,8-naphthaleneimide, pyrene)-sterically hindered amine (HAS). For all types of probes, the formation of the triplet state with absorption in the range 400–500 nm occurred after 266 nm excitation. The same triplet was formed at 355 nm excitation for probes extending absorption to this region. Triplet states of all probes were quenched by oxygen with rate constant $1–5 \times 10^9$ dm^3 mol^{-1} cm^{-1}. Intermolecular quenching of triplet states of the parent probes by *N*-oxyl (1-oxo-2,2,6,6-tetramethyl-4-hydroxypiperidine) was effective for naphthalene type probes and practically no effective for pyrene ones. The efficiency of intramolecular quenching in oxidised probes was determined by type of chromophore. The most effective intramolecular quenching was observed for *N*-(1-oxo-2,2,6,6-tetramethyl-4-piperidinyl)-1,8-naphthaleneimide in methanol.

Keywords: *N*-oxyl; Sterically hindered amine (HAS); Triplet route

1. Introduction

Free radicals of the *N*-oxyl type attract attention for several reasons. They play an important role in the course of stabilisation of polymers, mainly polyolefins, by sterically hindered amines since each molecule is able to break several radical chains behaving as “inhibition catalysts” [1,2]. This feature has been explained with the ability of the aminoethers to convert back to nitroxyls by reacting with alkylperoxy radicals. This regenerative step has been recently analysed experimentally and theoretically [3,4].

Secondly, the free radicals influence the photophysical and photochemical processes due to their paramagnetic effect [5–13]. Quenching of singlet and triplet states of aromatic hydrocarbons and ketones was studied in detail.

In the early nineties fluorescence probes were prepared in which simple aromatic chromophore was combined with a free radical centre of the *N*-oxyl type. Formation or decay of the free radical is connected with switching off or on of the chromophore emission as a result of intramolecular quenching [14].

Mechanism of inter or intramolecular quenching of excited states by *N*-oxyls is not unequivocally established. The following processes are discussed.

- Catalytic enhancement of intersystem crossing as a result of an increase in spin-orbital coupling due to the paramagnetic effect.
- Catalytic enhancement of the efficiency of internal conversion.
- Transfer of electronic energy of resonance or exchange type.
- Transfer of electron and formation of cation or anion radical.

The majority of mechanistic studies of quenching of the singlet state of aromatic hydrocarbons with *N*-oxyl radicals concluded that enhancement of intersystem crossing is the most probable route for dissipation of energy. Quenching of a triplet state occurs through internal conversion [5–13]. The photophysical process is a preferred route for deactivation of excited state by intramolecular quenching as well [14].

On the other hand, the photoinitiated intramolecular electron transfer from *N*-oxyl to diimide under formation of diimide monoanion has been observed recently [15]. These studies indicate that *N*-oxyl radical is able to quench the

* Corresponding author. Tel.:+421-754773448; fax: +421-754775923.
E-mail address: upolhrdl@savba.sk (P. Hrdlovič).

1010-6030/01/$ – see front matter
PII: S1010-6030(00)00376-2

excited state by different mechanisms depending on the structure of the couple quenchee–quencher and medium.

Recently time-resolved electron spin resonance (TR-EPR) has been used to investigate the chemically induced dynamic electron polarisation (CIDEP) generated between a *N*-oxyl and the triplet state of thioxanthonedioxide derivatives, which is in a molecules where these moieties are covalently linked [16]. Two mechanisms have been proposed to explain the quenching of the triplet state by *N*-oxyl radical. One is radical triplet pair mechanism and another is electron spin polarisation transfer.

Scaiano et al. [17] explored the possibility of the reversed process namely the photosensitised decomposition of aminoethers as potential methods for the initiation of "living" free radical polymerisation through *N*-oxyls. Such decomposition can facilitate this polymerisation at lower temperatures. It was concluded that triplet sensitisers with triplet level near 290 kJ mol^{-1} (index) would be required for efficient quenching and formation of free *N*-nitroxyl radicals to control polymerisation.

In this paper the triplet route of deactivation has been explored for probes of aromatic hydrocarbon/amine and aromatic hydrocarbon/*N*-oxyl with naphthalene, 1,8-naphthaleneimide and pyrene in solution. The intermolecular quenching of probes with parent amine and related compounds by *N*-oxyls was compared with intramolecular quenching. The probes were prepared previously and their spectral properties originating in the singlet state have been examined [18–23].

2. Experimental

Solvents such as methanol, cyclohexane, chloroform and methylene dichloride were used for UV spectroscopy. Naphthalene and pyrene (Lachema Brno, CR) were zonally refined. The free radicals 1-oxo-2,2,6,6-tetramethyl-4-hydroxypiperidine (Q1) m.t.: 68–69°C, and 1-oxo-2,2,6,6-tetramethyl-4-piperidinyl stearate (Q2) m.t.: 37–39°C were the same as in [24].

The structure of probes used in this paper is shown on Schemes 1, 2 and 3. Their preparation has already been partly described [18–22]. The details of the synthesis of probes based mainly on pyrene will be given elsewhere [23]. They were prepared by using standard procedures of organic synthesis as in [21,22]. Here, some spectral data are given for those compounds, which have not yet been prepared [23].

The following probes based on naphthalene as chromophore (Scheme 1) were used [18]: 2,2,6,6-tetramethyl-4-piperidinyl(1-naphthoate)ium chloride (N2) m.t: 246–249°C, 1-oxo-2,2,6,6-tetramethyl-4-piperidinyl-1-naphthoate (N3) mp 99–101°C, 2,2,6,6-tetramethyl-4-piperidinyl-1-naphthoylamide (N4) m.t: 205.5–206.5°C, 1-oxo-2,2,6,6-tetramethyl-4-piperidinyl-1-naphthoylamide (N5) m.t: 193–196°C, 2,2,6,6-tetramethyl-4-piperidinyl(1-naphthylacetate)ium chloride (N6) m.t: 268°C (decomposition),

	R_1	R_2	m. t.	Ref.
N1	H			
N2	$COOR_2$	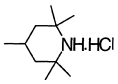	246 - 249°C	18
N3			99- 101°C	18
N4	$CONHR_2$		205. 5 - 206,5°C	
N5		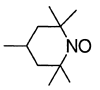	193 - 196°C	18
N6	CH_2COOR	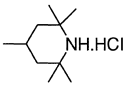	268°C (decomposition)	18
N7		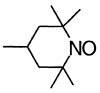	39 – 41 °C	
N8	CH_2CONHR_2	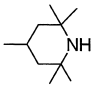	143 – 145 °C	
N9		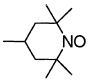	144 – 147 °C	

Scheme 1.

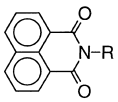

	R_1	R_2	m. t.	Ref.
NI1	$(CH_2)_{17}CH_3$		48 – 50°C	20
NI2	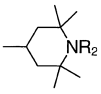	- H	168 – 170°C	20
NI3		- O	227 – 229°C	20
NI4		$-OCOCH_3$	186 – 188°C	20
NI5		$-CO\,CH_3$	200 – 201°C	20
NI6		- H.HCl	>250 decomposition	20
NI7		- OH	224 - 228°C	20

Scheme 2.

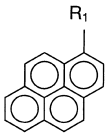

	R1	R2	m. t.	Ref.
P1	H			
P2	- $CH_2CH_2CH_2COOR_2$	- H		
P3		- CH_3	47 - 51°C	21
P4			liquid	21
P5			110 - 112°C	22
P6		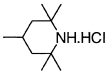		21
P7	- CH_2COOR_2	- CH_3	99 - 92°C	23
P8			35 – 40°C	23
P9			47 – 50°C	23
P10	- COOR	- CH_3		23
P11			126 – 128°C	23
P12			174- 176°C	23
P13	- $COCH_2CH_2COOR_2$	- CH_3	104 – 108°C	23
P14			121,5 – 123°C	23
P15			95 - 99°C	23

Scheme 3.

1- oxo-2, 2,6,6- tetramethyl- 4-piperidinyl-1-naphthylacetate (N7) m.t: 39–41°C, 2,2,6,6-tetramethyl-4-piperidinyl 1-naphthylacetamide (N8) m.t: 143–145°C, 1-oxo-2,2,6,6-tetramethyl-4-piperidinyl-1-naphthylacetamide (N9) m.t: 144–147°C.

The probes with 1,8-naphthaleneimide as chromophore (Scheme 2) are [19,20]: *N*-octadecyl-1,8-naphthaleneimide (NI1) m.t: 48–50°C, *N*-(2,2,6,6-tetramethyl-piperidin-4-yl)-1,8-naphthaleneimide (NI2) m.t: 168–170°C, *N*-(1-oxo-2,2,6,6-tetramethylpiperidin-4-yl)-1,8-naphthaleneimide (NI3) m.t: 227–229°C, *N*-(1-acetyloxy-2,2,6,6-tetramethylpiperidin-4-yl)-1,8-naphthaleneimide (NI4) m.t: 186–188°C, *N*-(1-acetyl-2,2,6,6-tetramethylpiperidin-4-yl)-1,8-naphthaleneimide (NI5) m.t: 200–201°C, *N*-(2,2,6,6-tetramethylpiperidin-4-yl)-1,8-naphthaleneimide)ium chloride (NI6) m.t: >250°C (decomposition), *N*-(1-hydroxy-2,2,6,6-tetramethylpiperidin-4-yl)-1,8-naphthaleneimide (NI7) m.t: 224–228°C.

The pyrene based probes (Scheme 3) are [21,22]: 4-(1-pyrene)butyric acid (P2), (Aldrich–Chemie, Steinheim, FRG), methyl-4-(1-pyrene)butyrate (P3) m.t: 47–51°C, 2,2,6,6-tetramethyl-4-piperidinyl-4-(1-pyrene)butyrate (P4), liquid, 1-oxo-2,2,6,6-tetramethyl-4-piperidinyl-4-(1-pyrene) butyrate (P5) m.t: 110–112°C, (2,2,6,6-tetramethyl-4-piperidinyl 4-(1-pyrene)butyrate)ium chloride (P6) m.t: 220–230°C.

The novel series of pyrene based probes include [23]: methyl-1-pyreneacetate (P7) mp 90–92°C, 2,2,6,6-tetramethyl-4-piperidinyl-1-pyreneacetate (P8), m.t: 35–40°C, ^{1}H NMR ($CDCl_3$) δ: 1,2 (s, 6H, 2 × CH_3, 2 + 6 axial) 1,25 (s, 6H, 2 × CH_3, 2 + 6 equat) 1,3 (m, 2H, CH_2, 3 + 5 axial) 1,9 (m, 2H, CH_2, 3+5 equat) 4,3 (s, 2H, CH_2CO) 5,2 (m, 1H, CH–O) 7,95–8,3 (m, 9H, pyrene), FTIR ($CHCl_3$) (cm^{-1}): ν(C=O) 1724, ν(C–N) 1370, ν(C–O) 1165, ν(pyrene) 847, UV (λ (nm) (log ε) in methanol): 233(4,64), 243(4,81), 255(4,02), 265(4,36), 276(4,62), 312(4,00), 325(4,39), 341(4,56), 1-oxo-2,2,6,6-tetramethyl-4-piperidinyl-1-pyreneacetate (P9), mp 47–50°C, FTIR ($CHCl_3$) (cm^{-1}): ν(C=O) 1727, ν(C–N) 1366, ν(C–O) 1163, ν(pyrene) 847, UV (methanol): 234(4,52), 243(4,75), 255(4,00), 265(4,29), 276(4,55), 311(3,95), 325(4,32), 341(4,49), methyl-1-pyrenoate (P10) mp 81–83°C, 2,2,6,6-tetramethyl-4-piperidinyl-1-pyrenoate (P11) mp 126–128°C, ^{1}H NMR ($CDCl_3$) δ: 1,37 (s, 6H, 2 × CH_3, 2 + 6 axial); 1,45 (s, 6H, 2 × CH_3, 2 + 6 equat); 1,59 (m, 2H, CH_2, 3 + 5 axial); 2,25 (m, 2H, CH_2, 3 + 5 equat); 5,66 (m, 1H, CH–O); 8,07–8,26 (m, 7H, 3–9 pyrén); 8,62 (d, 1H, 2 pyrene); 9,28 (d, 1H, 10 pyrene), FTIR ($CHCl_3$) (cm^{-1}) : ν(C=O) 1713, ν(C–O) 1194, ν(pyrene) 711, UV (methanol): 244(4,67), 273(4,34), 281(4,43), 352(4,37), 386(3,87), 1-oxo-2,2,6,6-tetramethyl-4-piperidinyl-1-pyrenoate (P12), mp 174–176°C, FTIR ($CHCl_3$) (cm^{-1}): ν(C=O) 1715, ν(C–O) 1198, ν(pyrene) 711, UV (methanol): 244(4,71), 270(4,45), 281(4,53), 352(4,37), 385(3,87), methyl-3-(1-pyrenoyl)propionate (P13) mp 104–108°C, 2,2,6,6-tetramethyl-4-piperidinyl-3-(1-pyrenoyl)propionate (P14), mp 121.5–123°C, ^{1}H NMR ($CDCl_3$) δ: 1,15 (s, 6H, CH_3, 2 + 6 axial); 1,25 (s, 6H, CH_3, 2 + 6 equat); 1,1–1,3 (m, 3H, CH_2, 3 + 5 axial +NH); 1,97 (m, 2H, CH_2, 3 + 5 equat); 2,9 (t, 2H, CH_2, CH_2–CO–); 3,55 (t, 2H, CH_2, CH_2–CO–O); 5,27 (m, 1H, >CH–O); 8,0–8,9 (m, 9H, pyrene), FTIR (KBr) cm^{-1}: ν(C–H) 3042–2900, ν(C=O) 1733, ν(C=O) 1674, ν(C–O) 1261, ν(pyrene) 852, UV (methanol): 234(4,52), 242(4,56), 281(4,44), 354(4,13), 1-oxo-2,2,6,6-tetramethyl-4-piperidinyl-3-(1-pyrenoyl)propionate (P15), m.t.: 95–99°C, IR (KBr) cm^{-1}: ν(C=O) 1733, ν(C=O) 1672, ν(NO) 1363, ν(C–O) 1155, ν(pyrén) 849, UV (methanol): 234(4,60), 242(4,62), 281(4,46), 353(4,19).

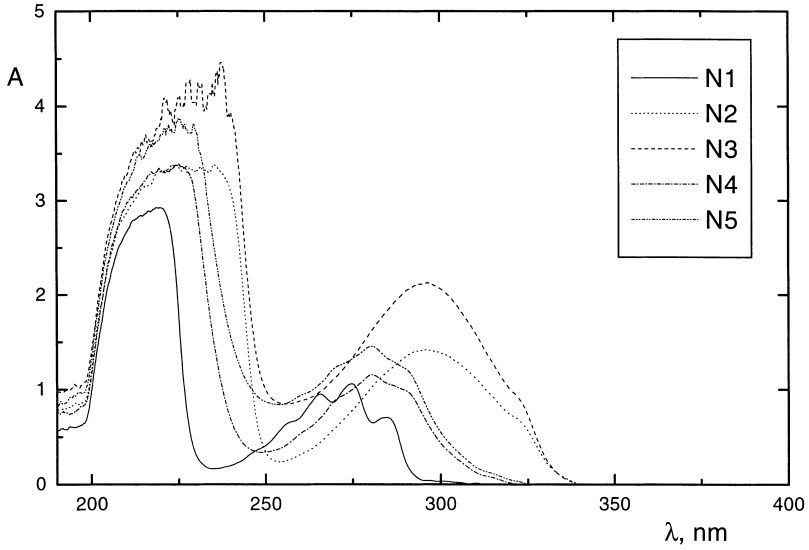

Fig. 1. Absorption spectra of probes N1–N5 in methanol.

Absorption spectra were recorded on M40 (C. Zeiss, Jena, FRG) and on UV 160 (Shimadzu, Japan).

Transient absorption spectra in the time scale 20 ns to 500 μs were carried out on a nanosecond laser flash photolysis LKS 60 from Applied Photophysics Ltd (London, England). The laser excitation at 266 nm (fourth harmonic) and 355 nm (third harmonic) from Quanta Ray GCR 130-1 Nd:YAG (pulse width ∼9 ns) was used in right angle geometry with respect to the monitoring light beam. The transient absorbances at preselected wavelength were monitored by a detection system composed of a pulsed xenone-lamp (150 W), monochromator and a 1P28 photomultiplier. A unit controlled synchronising of the pulse lamp, programmable shutters and high voltage power supply with laser output. The signal from photomultiplier was displayed on digital osciloscope (HP 54522A) and analysed on 32 bit RISC work station [25].

3. Results and discussion

3.1. Naphthalene based probes

At excitation with 266 nm pulses esters and amides of 1-naphthoic or 1-naphthylacetic acids with 2,2,6,6-tetramethyl-4-hydroxypiperidine or 2,2,6,6-tetramethyl-4 aminopiperidine (Scheme 1, N2–N9) are excited between intense absorption below 250 nm and longest wavelength band above 275 nm (Figs. 1 and 2). For derivatives of 1-naphthoic acid (N2–N5), this band exhibits maximum shifted up to

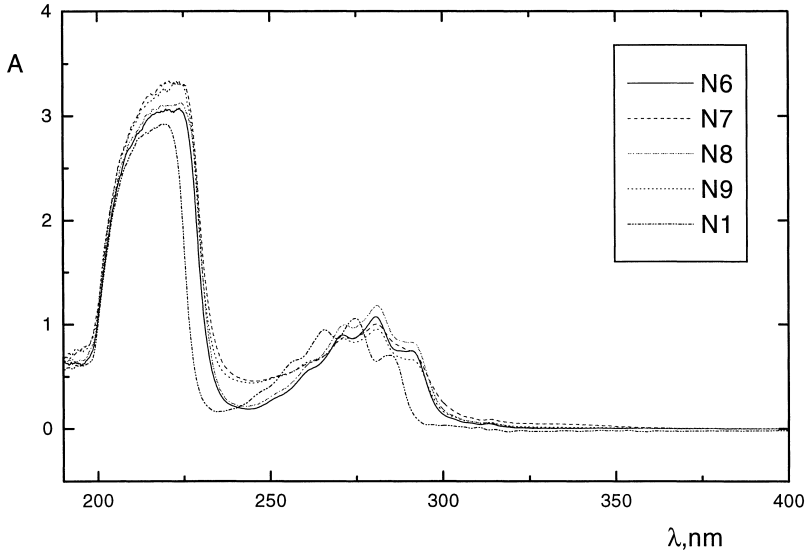

Fig. 2. Absorption spectra of probes N1 and N6–N9 in methanol.

Table 1
Kinetic data for the decay of probes based on naphthalene

Probe[a]	Cond.[b]	λ[c] (nm)	F[d]	k[e] (s^{-1})	τ[f] (μs)	k_q[g] ($dm^3 mol^{-1} s^{-1}$)	k_{NO}/k_{NH}[h]
N1	Air	400	M	3.58×10^6	0.28	1.63×10^9	
	N_2	415	M	6.77×10^4	14.8		
	Q1/N_2	415	M	3.69×10^5		1.50×10^9	
N2	Air	430	M	2.32×10^6	0.43	1.05×10^9	
	N_2	415	M	3.42×10^4	29.2		
N3	Air	415	M	2.60×10^6			76
	N_2			weak signal			
N4	Air	415	M	2.65×10^6	0.38		
	N_2	430	M	1.77×10^4	56.5	1.20×10^9	
N5	Air	415	M	3.90×10^6	0.26		
	N_2	415	M	1.13×10^6	0.88		63.8
N6	Air	410	M	2.98×10^6	0.34	1.35×10^9	
	N_2	410	M	3.46×10^4	28.9		
			B	1.02×10^5 (47%)			
				2.03×10^4 (53%)			
	Q1/N_2	410		1.29×10^5		6.0×10^8	
N7	Air	410	B	6.41×10^6 (85%)			
				5.21×10^5 (15%)			
	N_2	410	B	5.68×10^5 (65%)			
				2.62×10^4 (35%)			
	N_2	410	M	4.74×10^5 fast			13.7
				2.46×10^4 slow			
N8	Air	410	M	3.32×10^6	0.30	1.51×10^9	
	N_2	410	M	4.57×10^4	21.9		
		410	B	2.28×10^5 (86%)			
				8.46×10^3 (14%)			
	Q1/N_2	410	M	1.82×10^5		6.82×10^8	
N9	Air	410	M	3.54×10^6			
	N_2	410	M	6.71×10^5			14.6

[a] Structure of the probes according to Scheme 1.
[b] Experimental conditions: air-aerated solution: methanol (O_2) = 2.2×10^{-3} mol dm^{-3}; N_2 bubbling with stream of nitrogen for 10 min, Q1 = 2×10^{-4} mol dm^{-3} (1-oxo-2,2,6,6-tetramethyl-4-hydroxypiperidine).
[c] Monitoring wavelength.
[d] Fitting to monoexponential, M or biexponential, B.
[e] Rate constant of decay.
[f] Life-time of the excited state.
[g] Bimolecular rate constant of quenching by oxygen and Q1.
[h] Ratio of the rate constant of the oxidised and parent probe.

300 nm without any vibrational structure. Derivatives of 1-naphthylacetic acid (N6–N9) are in fact excited in the longest wavelength band with distinct vibrational structure. In this way in both structures the singlet state is generated which transforms in triplet state in certain fraction.

Transient absorption around 400 nm of naphthalene and other probes (N2–N9) as well belongs to triplet absorption. This absorption decays as monoexponential very fast in the presence of oxygen. Kinetic data obtained from decay curves for naphthalene derivatives are given in Table 1. The concentration of oxygen in the air saturated methanol or cyclohexane is in the range 2.2×10^{-3} mol dm^{-3} [26]. On the other hand, the decay of this absorption is two orders of magnitude slower in deaerated solutions. The transient absorption of all probes of this type with parent amine (N2, N4, N6, N8) is similar to that of naphthalene (Fig. 3). The decay of transient absorption of these probes containing parent amine fits better double exponential than monoexponential. Especially the beginning of the decay is faster as it should be according to monoexponential. In order to compare intermolecular with intramolecular quenching, a model quencher as 1-oxo-2,2,6,6-tetramethyl-4-hydroxypiridine (Q1) was used. Moreover, the 1-oxo-2,2,6,6-tetramethylpiperidine moiety is part of the more complex probe for testing the intramolecular quenching. For naphthalene the bimolecular rate constant of quenching with Q1 is comparable with the rate constant of oxygen. In quenching of naphthalene triplet state both quenching rate constants for Q1 and O_2 are lower by an order of magnitude than the diffusion limited bimolecular rate constant 1–2 $\times 10^{10}$ dm^3 mol^{-1} s^{-1}. The ratio of the decay

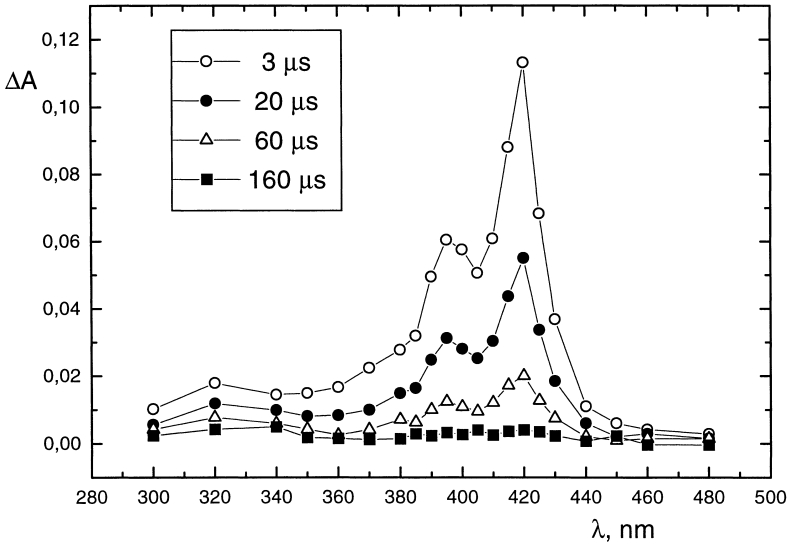

Fig. 3. Transient absorption spectra of N6 in methanol at 266 nm excitation.

rate constants for oxidised and parent amine k_{NO}/k_{NH} for couples N3/N2 and N5/N4 indicates that the intramolecular quenching is very effective. The ratio k_{NO}/k_{NH} lies in the range 60–80. For probe N3 the transient absorption is rather weak and its decay is fast. For N5 the decay is even more rapid. The life-time is shorter than 400 ns. Probes derived from 1-naphtylacetic acid exhibit less effective intermolecular quenching with Q1 as compared with oxygen. The ratio of k_{NO}/k_{NH} is lower in the range 10–15 indicating less effective intramolecular quenching as well. It looks like that the presence of one methylene bridge inhibits the efficiency of the intramolecular quenching (or intramolecular deactivation) of the triplet state.

3.2. 1,8-Naphthaleneimide based probes

With 266 nm (fourth harmonic) pulses the excitation of probes with 1,8-naphthaleneimide chromophore occurs in minimum between two bands (Fig. 4). At 355 nm excitation (third harmonic) the excitation at the long wavelength edge of the first band takes place. This excitation occurs more effectively in methanol solution where the absorption band is broader and red shifted than in cyclohexane where this band is blue shifted and better vibrationally resolved (Fig. 5). Oxidation of the parent sterically hindered amine (NI2) to stable nitroxyl radical (NI3) and its reduction to hydroxylamine (NI7) does not influence the absorption spectrum.

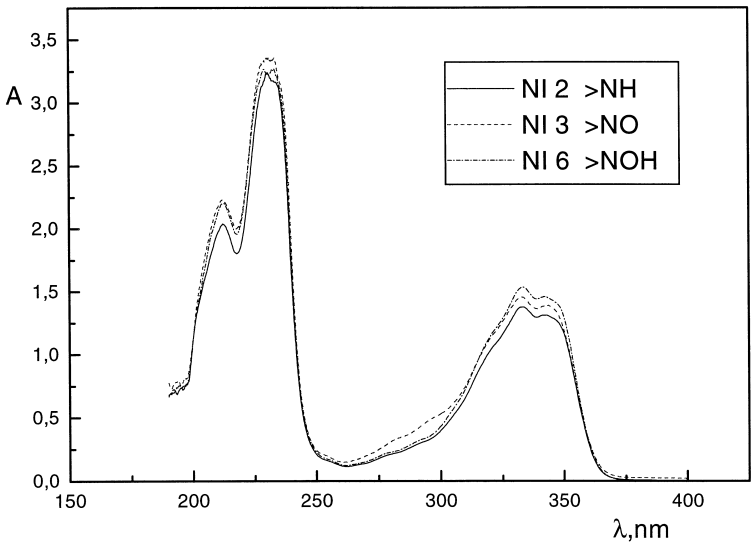

Fig. 4. Absorption spectra of probes NI2, NI3 and NI6 in methanol.

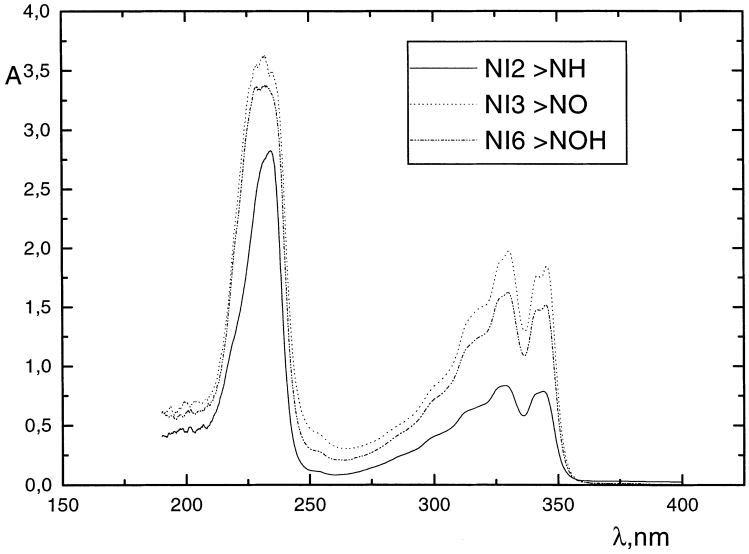

Fig. 5. Absorption spectra of probes NI2, NI3 and NI6 in cyclohexane.

The decay of transient absorption of NI1 and NI2 at 266 nm excitation in methanol is about 50 up to 100 times more rapid in the presence of oxygen around $1 \times 10^6\,s^{-1}$ (Table 2) as in atmosphere of N_2 ($1–5 \times 10^4$). For NI3 no transient was observed in the presence of oxygen as well as in nitrogen atmosphere. It means that the process of intramolecular quenching with *N*-oxyl for this probe is rather fast. Since the decay process with rate constant about $10^7\,s^{-1}$ is easy to measure in this set up, the life-time of the excited state is shorter than 100 ns. Triplet state of NI1 and NI2 is quenched with Q1 as well with the rate slightly higher than with oxygen. Using NI3 as a intermolecular quencher the process is even more rapid ($k_q \sim 4–5 \times 10^9\,dm^3\,mol^{-1}\,s^{-1}$). In this case the used probe NI3 quenches first itself because it absorbs 266 nm light as NI2 (see Fig. 5) and after then it quenches excited states of NI1 and NI2, respectively. This points out on the extremely fast quenching occurring in NI3. Transient absorption of NI1 and NI2 probes exhibits maximum at 470 nm with 266 nm excitation in methanol (Fig. 6). At 410 nm there is a transient which decays distinctly slower indicating different structure (possibly cation radical). Since at 266 nm there is some absorption of Q1 at higher concentration above $10^{-3}\,mol\,dm^{-3}$ and some other effects besides screening could take place, the 355 nm excitation at the

Table 2
Kinetic data of decay of transient absorption of probes based on 1,8-napthaleneimide in methanol at 266 nm excitation

Probe[a]	Cond.[b]	λ[c] (nm)	F[d]	k[e] (s^{-1})	τ[f] (μs)	k_q[g] ($dm^3\,mol^{-1}\,s^{-1}$)	k_{NO}/k_{NH}[h]
NI1	Air	410	M	1.60×10^6	0.625	7.3×10^8	
	N_2	410	M	9.92×10^3	100.8		
	Q1/N_2	470	M	2.28×10^5		2.2×10^9	
	NI3/N_2	470	M	2.90×10^5		4.9×10^9	
NI2	Air	470	M	2.46×10^6	0.413	1.1×10^9	
	N_2	470	M	5.09×10^4	19.6		
	Q1/N_2	470	M	1.75×10^5		1.2×10^9	
	NI3/N_2	470	M	2.71×10^5		4×10^9	
NI3				No transient			

[a] Structure of the probes according to Scheme 2.
[b] Experimental conditions: air-aerated solution: methanol (O_2) = 2.2×10^{-3}mol dm^{-3}; N_2 bubbling with stream of nitrogen for 10 min, Q1 = 10^{-4}mol dm^{-3} (1-oxo-2,2,6,6-tetramethyl-4-hydroxypiperidine) NI3 (quencher).
[c] Monitoring wavelength.
[d] Fitting to monoexponential, M or biexponential, B.
[e] Rate constant of decay.
[f] Life-time of the excited state.
[g] Bimolecular rate constant of quenching by oxygen, Q1 and NI3 (4.5×10^{-4}).
[h] Ratio of the rate constant of the oxidised and parent probe.

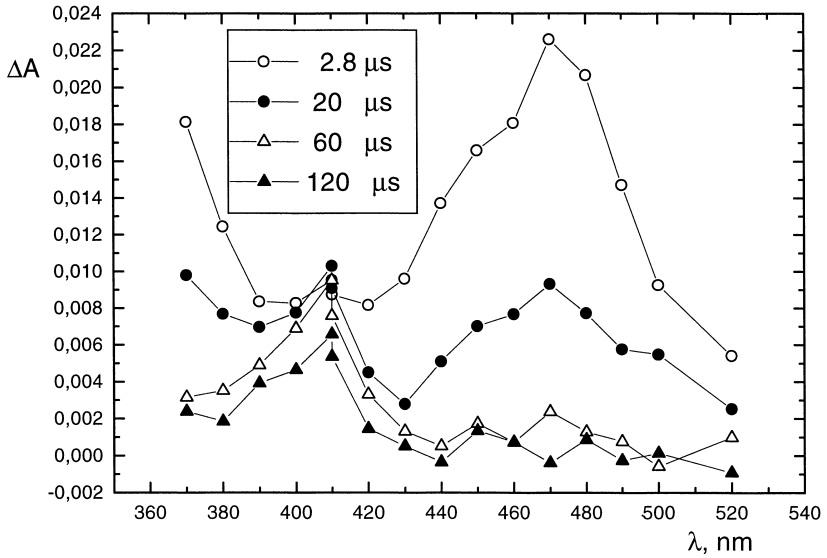

Fig. 6. Transient absorption spectrum of NI2 in deaerated methanol at 266 nm excitation.

long wavelength edge was employed. At 355 nm excitation the spectra of the transient has got the same feature as at 266 nm (Fig. 7) with maximum at 470 nm and slow decay at 410 nm. The transient spectrum is nearly the same for all *N*-(1-substitted-2,2,6,6-tetramethyl-4-piperidyl)-1,8-naphthalenimides at 355 nm excitation with exception of 1-oxo derivatives (NI3). Although the transient of NI3 at 355 nm was weak, but some signal was observed probably because excitation at this wavelength was about three times more intense than at 266 nm. The decay was composed from two parts, faster with the rate constant $3.5 \times 10^7\,s^{-1}$ and slower with $1 \times 10^6\,s^{-1}$. In the initial phase the intramolecular quenching is about 600 times more effective but in later phase the efficiency is lower. At 355 nm excitation, the transient absorption for all 1,8-naphthalene probes decays fast in aerated solutions and slower in deaerated solutions as at 266 nm (Table 3). Bimolecular rate constant of quenching with O_2 is $1 \times 10^9\,dm^3\,mol^{-1}\,s^{-1}$ and for Q1 slightly higher $1.5–2 \times 10^9\,dm^3\,mol^{-1}\,s^{-1}$. As with probes based on naphthalene, quenching with Q1 and O_2 is well below diffusion controlled limit for these types of probes as well. The decays of transient absorption fit monoexponential but in nitrogen atmosphere the decay is better described by biexponential with fast rate $2 \times 10^5\,s^{-1}$ and slow rate $4 \times 10^4\,s^{-1}$. The transient spectra with 1,8-naphthleneimide chromophore at 355 nm in cyclohexane exhibit the same features as in

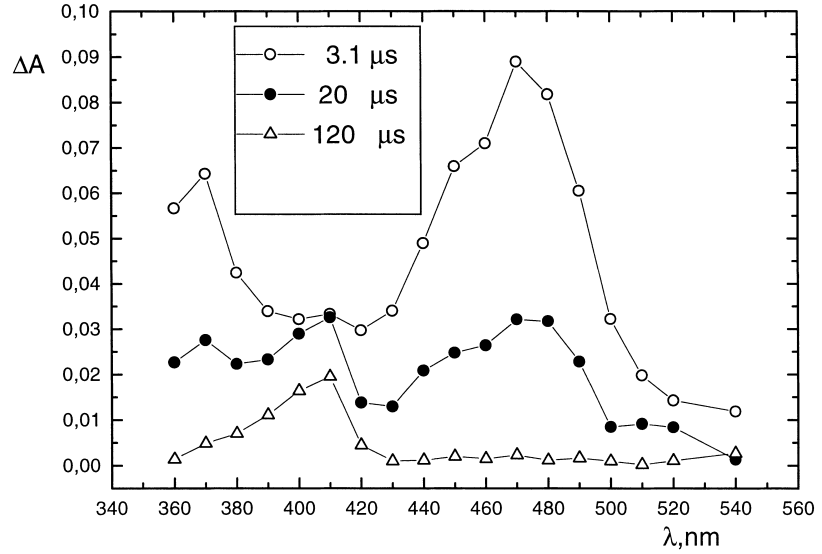

Fig. 7. Transient absorption spectrum of NI2 in deaerated methanol at 355 nm excitation.

Table 3
Kinetic data of decay of 1,8-naphthaleneimide based probes in methanol at 355 nm excitation

Probe[a]	Cond.[b]	λ[c] (nm)	F[d]	k[e] (s^{-1})	τ[f] (μs)	k_q[g] $dm^3\,mol^{-1}\,s^{-1}$	k_{NO}/k_{NH}[h]
NI1	Air	470	M	2.39×10^6	0.42	1.1×10^9	
	N_2	470	M	9.81×10^4	10.2		
		470	B	2.39×10^5 (71%)	2.71		
				4.20×10^4 (29%)			
	Q1/N_2			2.62×10^5		1.64×10^9	
NI2	Air	470	M	2.09×10^6	0.48	0.95×10^9	
	N_2	470	M	5.60×10^4			
			B	1.15×10^5 (62%)			
				2.92×10^4 (38%)			
	Q1/N_2			1.73×10^6		1.67×10^9	
NI3	Air	470	M	2.80×10^7	0.04	3.2×10^9	
	N_2	470	M	3.51×10^7 fast	0.03		627
		470	M	1.06×10^6 slow	0.94		19
NI4	Air	470	M	2.19×10^6	0.46	9.96×10^8	
	N_2	470	M	4.06×10^4	24.6		
			B	1.07×10^5 (54%)			
				2.35×10^4 (46%)			
	Q1/N_2	470		1.61×10^6		1.56×10^9	
NI5	Air	470	M	2.20×10^6	0.46	1.1×10^9	
	N_2	470	M	9.75×10^4	10.3		
		470	B	2.25×10^5 (69%)			
	Q1/N_2	470	M	4.63×10^4 (31%)			
				2.06×10^6		1.97×10^9	
NI6	Air	470	M	2.16×10^6	0.46	0.98×10^9	
	N_2	470	M	7.49×10^4	13.4		
			B	1.56×10^5 (64%)			
				3.79×10^4 (36%)			
	Q1/N_2	470	M	2.23×10^6		2.16×10^9	
NI7	Air	470	M	2.18×10^6	0.46	0.99×10^9	
	N_2	470	M	7.28×10^4	13.7		
				1.79×10^5 (66%)			
				4.03×10^4 (34%)			
	Q1/N_2			1.98×10^6		1.91×10^9	

[a] Structure of the probes according to Scheme 2.
[b] Experimental conditions: air-aerated solution: methanol (O_2) = 2.2×10^{-3} mol dm^{-3}; N_2 bubbling with stream of nitrogen for 10 min, Q1 = 10^{-3} mol dm^{-3} (1-oxo-2,2,6,6-tetramethyl-4-hydroxypiperidine).
[c] Monitoring wavelength.
[d] Fitting to monoexponential, M or biexponential, B.
[e] Rate constant of decay.
[f] Life-time of the excited state.
[g] Bimolecular rate constant of quenching by oxygen and Q1.
[h] Ratio of the rate constant of the oxidised and parent probe.

methanol (Fig. 8) having maximum at 470 nm. The shoulder at 440 is more pronounced and long living intermediate at 410 is less clear. The kinetic data of decay in O_2 and N_2 in cyclohexane are nearly the same as in methanol (Table 4). The quenching rate constants for Q1 and O_2 are for the most of the probes similar in cyclohexane and in methanol. Therefore, no solvent effect is observed on the decay of transient absorption for most of the probes except NI3 and NI7. The intramolecular quenching in NI3 is one order less effective in cyclohexane ~50 as compared with methanol ~600. The other exception is NI7 (*N*-1-hydroxy derivative) which exhibits similar decay in deaerated methanol as other derivatives but rather fast decay in cyclohexane. Decay in aerated solution is roughly two times faster as for other probes. In inert atmosphere of nitrogen the difference of the decay is even more pronounced and represents roughly one order. Probably, some partial oxidation of NI7 to NI3 cannot be completely excluded in non polar cyclohexane, but why it does not happen in methanol is not clear.

3.3. Pyrene based probes

Using 266 nm pulses the excitation is directed between $S_0 \rightarrow S_3$ and $S_0 \rightarrow S_4$ absorption bands for probes containing

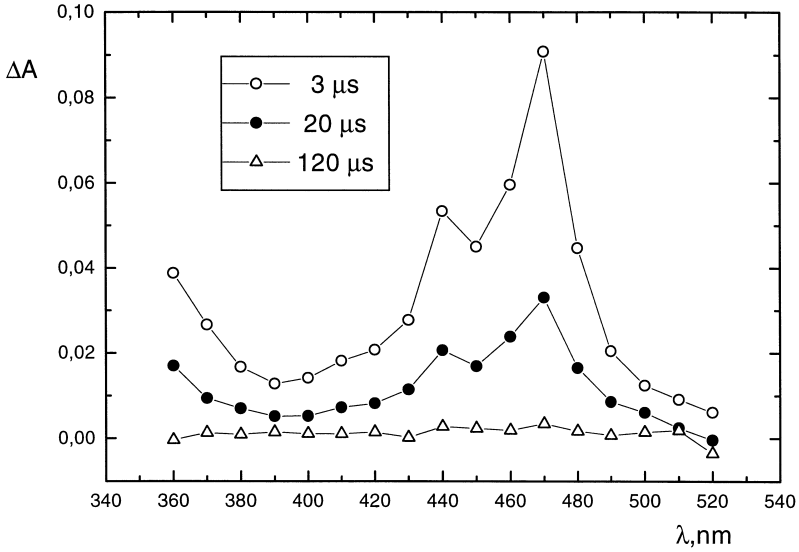

Fig. 8. Transient absorption spectrum of N14 in deaerated cyclohexane at 355 nm.

1-alkyl chromophore such as P1–P9 (Fig. 9). For probes containing carbonyl group in α-position to pyrene (1-pyrenoyl or 1-pyrenecarboxyl) such as P10–P15 excitation is located in short wavelength part of the band $S_0 \rightarrow S_3$ (Fig. 10). For these probes the longest band wavelength is shifted to 400 nm and therefore, the 355 nm pulses can be employed as well. Using both types of excitation, the triplet state of substituted pyrene is formed causing transient absorption. The

Table 4
Kinetic data of decay of 1,8-naphthaleneimide based probes in cyclohexane at 355 nm excitation

Probe[a]	Cond.[b]	λ[c] (nm)	F[d]	k[e] (s^{-1})	τ[f] (μs)	k_q[g] ($dm^3\,mol^{-1}\,s^{-1}$)	k_{NO}/k_{NH}[h]
NI1	Air	470	M	2.59×10^6	0.39	1.8×10^9	
	N_2	470	M	1.27×10^5	7.9		
		470	B	3.43×10^5 (68%)			
				5.22×10^4 (32%)			
	$Q1/N_2$	470	M	1.28×10^6		1.15×10^9	
NI3	Air	470	M	8.85×10^6	0.11	1.1×10^9	48.1
	N_2	470	M	6.11×10^6	0.16		
NI4	Air	470	M	2.43×10^6	0.41	1.0×10^9	
	N_2	470	M	5.54×10^4	18.1		
			B	1.51×10^5 (61%)			
				2.73×10^4 (39%)			
NI5	Air	470	M	2.46×10^6	0.41	1.03×10^9	
	N_2	470	M	5.07×10^4	19.7		
		470	B	1.39×10^5 (60%)			
				2.44×10^4 (40%)			
	$Q1/N_2$			1.60×10^6		1.55×10^9	
NI7	Air	470	M	5.55×10^6	0.18	2.30×10^9	
	N_2	470	M	2.34×10^6	0.43		
	$Q1/N_2$	470	M	4.67×10^6		2.33×10^9	

[a] Structure of the probes according to Scheme 2. NI2 not included since it is insoluble.
[b] Experimental conditions: air-aerated solution: cyclohexane $(O_2) = 2.4 \times 10^{-3}\,mol\,dm^{-3}$; N_2 bubbling with stream of nitrogen for 10 min, Q1 = $10^{-3}\,mol\,dm^{-3}$ (1-oxo-2,2,6,6-tetramethyl-4-hydroxypiperidine).
[c] Monitoring wavelength.
[d] Fitting to monoexponential, M or biexponential, B.
[e] Rate constant of decay.
[f] Life-time of the excited state.
[g] Bimolecular rate constant of quenching by oxygen and Q1.
[h] Ratio of the rate constant of the oxidised and parent probe.

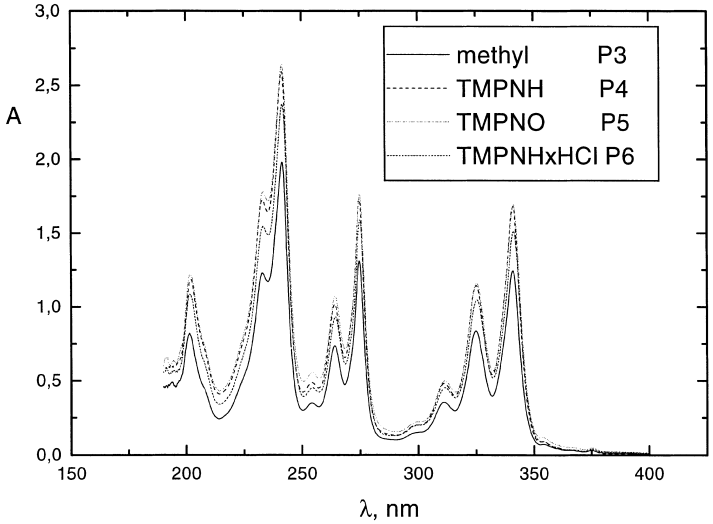

Fig. 9. Absorption spectra of derivatives of 4-(1-pyrene)butyric acid P3–P6 in methanol.

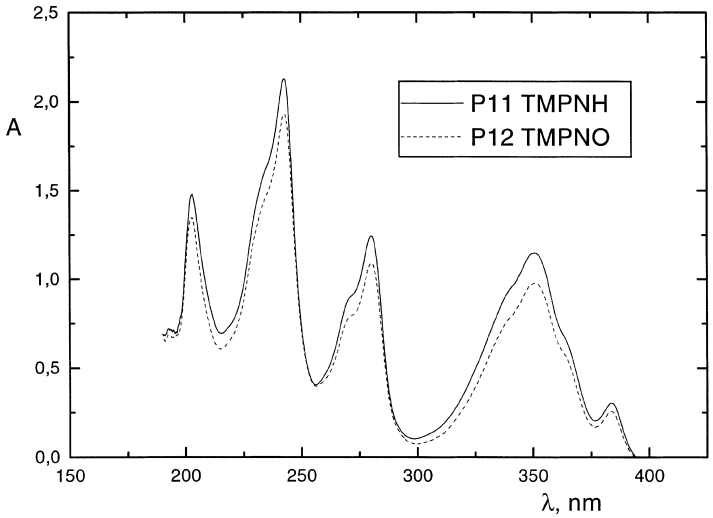

Fig. 10. Absorption spectra of derivatives of 1-pyrenecarboxylic acid P10–P12 in methanol.

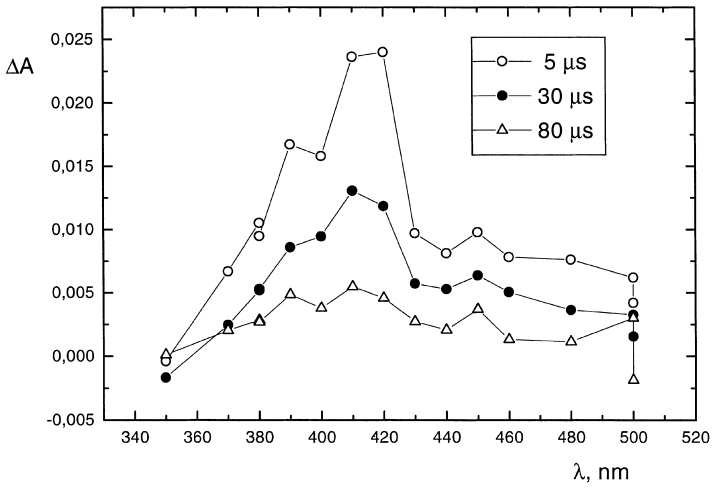

Fig. 11. Transient absorption spectrum of P4 in deaerated methanol at 266 nm excitation.

Table 5
Kinetic data of decay of probes pyrene-sterically hindered amine in methanol at 266 nm excitation

Probe[a]	Cond.[b]	λ[c] (nm)	F[d]	k[e] (s^{-1})	τ[f] (μs)	k_q[g] ($dm^3\,mol^{-1}\,s^{-1}$)	k_{NO}/k_{NH}[h]
P1	Air	400		4.67×10^6	0.21	2.1×10^9	
	N_2	410		3.18×10^4	31.4		
				7.88×10^4 (51%)			
				1.79×10^4 (49%)			
P2	Air	410	M	3.68×10^6	0.28	1.67×10^9	
	N_2	410	M	3.24×10^4	30.9		
P3	Air	410	M	4.88×10^6	0.21	2.22×10^9	
	N_2	410	M	3.11×10^4	32.2		
	Q_1/N_2	410	M	3.77×10^4		$\sim 5.2 \times 10^7$	
P4	Air	410	M	4.65×10^6	0.22	2.1×10^9	
	N_2	410	M	3.12×10^4	32.1		
P5	Air	410	M	4.60×10^6	0.22	2.1×10^9	3.7
	N_2	410	M	1.22×10^5			
P6	Air	410	M	4.43×10^6	0.23	2.2×10^9	
	N_2	410	M	1.85×10^4	54.1		
	Q_1/N_2			6.17×10^4		4.7×10^7	
P7	Air	410	M	4.74×10^6	0.21	2.15×10^9	
	N_2	410	M	3.11×10^4	32.2		
P8	Air	410		4.40×10^6	0.23	2.0×10^9	
	N_2	410		3.04×10^4	32.8	1.75×10^7	
	Q_1/N_2	410		4.73×10^4			
P9	Air	410	M	4.26×10^6	0.24	1.94×10^9	2.51
	N_2	410		7.64×10^4			
P10	Air	410	M	4.03×10^6	0.25	1.83×10^9	
	N_2	410	M	3.47×10^4	28.8		
P11	Air	410	M	3.78×10^6	0.27	1.72×10^9	
	N_2	410	M	2.30×10^4	43.5		
	Q_1/N_2	410	M	3.07×10^4		7.7×10^7	
P12	Air	410	M	4.52×10^6	0.22	2.1×10^9	
	N_2	410	M	3.59×10^4			1.55
		410	B	1.21×10^5 (31%)			5.26
				2.79×10^4 (69%)			1.20
P13	Air	410	M	4.58×10^6	0.22	2.07×10^9	
	N_2	410	M	4.80×10^4	20.8		
		410	B	1.26×10^5 (55%)			
				2.79×10^4 (45%)			
P14	Air	410	M	4.32×10^6	0.23	1.96×10^9	
	N_2	410	M	4.34×10^4			
		410	B	1.18×10^5 (50%)			
				2.64×10^4 (50%)			
P15	Air	410	M	4.56×10^6	0.22		
	N_2	410	M	8.03×10^4			1.85
			B	2.96×10^5 (38%)			2.58
				6.46×10^4 (62%)		2.07×10^9	2.44

[a] Structure of the probes according to Scheme 3.
[b] Experimental conditions: air-aerated solution: methanol (O_2) = 2.2×10^{-3} mol dm^3; N_2 bubbling with stream of nitrogen for 10 min, Q1 = 10^{-3} mol dm^{-3} (1-oxo-2,2,6,6-tetramethyl-4-hydroxypiperidine).
[c] Monitoring wavelength.
[d] Fitting to monoexponential, M or biexponential, B.
[e] Rate constant of decay.
[f] Life-time of the excited state.
[g] Bimolecular rate constant of quenching by oxygen and Q1.
[h] Ratio of the rate constant of the oxidised and parent probe.

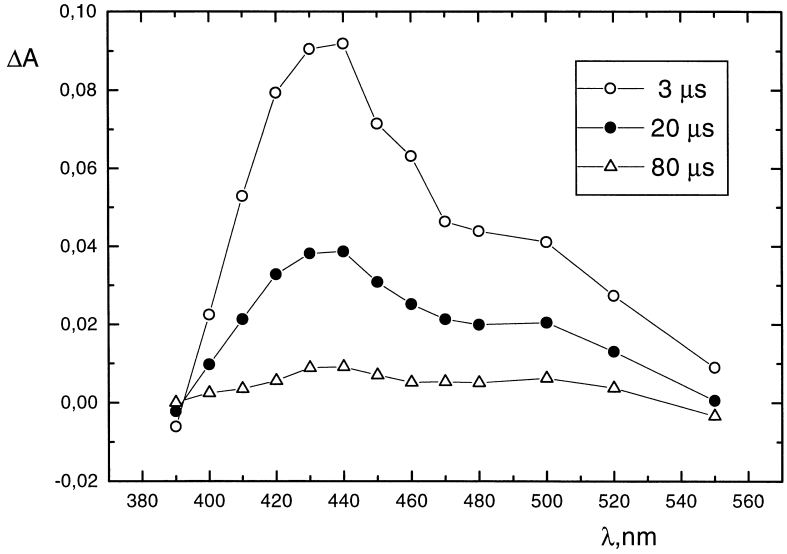

Fig. 12. Transient absorption spectrum of P14 in deaerated methanol at 266 nm excitation.

maximum of this transient absorption is around 410–420 nm with shoulder at 380–390 nm and less intense absorption at 440–450 nm. These features have got the transient spectrum in aerated and deaerated methanol of parent pyrene and probes P2–P9 (Fig. 11) (Table 5) at 266 nm excitation. For probes P10–P15 the transient spectrum is less resolved with maximum shifted up to 430 nm, no shoulder at 380–390 nm and weak absorption at 440–450 nm (Fig. 12). At 355 nm excitation the same transient absorption spectrum is observed for probes P10–P15 (Fig. 13) (Table 6).

Kinetic data obtained for unsubstituted pyrene and other pyrene based probes in aerated and deaerated methanol differ by two orders of magnitude. This is similar to other probes. The life-time in aerated solution is about 0.2 μs and in deaerated methanol about 30 μs. The probe P6 lives substantially longer. The rate constant of bimolecular quenching by O_2 is about $2 \times 10^9\,dm^3\,mol^{-1}\,s^{-1}$. Less efficient is intermolecular quenching of these probes with Q1 about $5 \times 10^7\,dm^3\,mol^{-1}\,s^{-1}$. The quenching with this radical was efficient for probes based on naphthalene and 1,8-naphthaleneimide. At the same time it might be expected that intramolecular quenching for probes with oxidised amine P5 and P9 will be weaker what is confirmed by the low value of k_{NO}/k_{NH} ~2 and 5 respectively. Nearly the same kinetic parameters were obtained for decay of transient absorption at 266 and 355 nm excitation for P10–P15. The intramolecular quenching is even less effective for these probes at 355 nm excitation about 1.5.

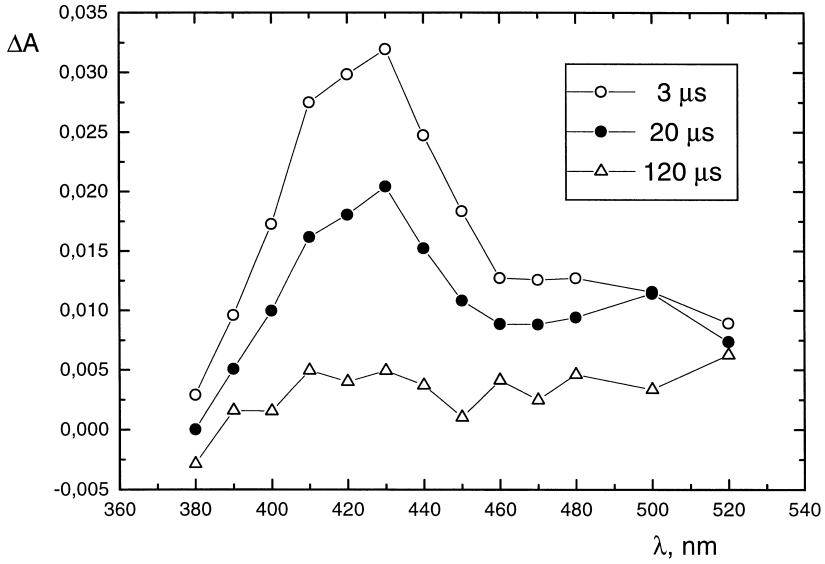

Fig. 13. Transient absorption spectrum of P11 in deaerated methanol at 355 nm excitation.

Table 6
Kinetic data of decay of probes pyrene-sterically hindered amine in methanol at 355 nm excitation

Probe[a]	Cond.[b]	λ[c] (nm)	F[d]	k[e] (s^{-1})	τ[f] (μs)	k_q[g] ($dm^3\,mol^{-1}\,s^{-1}$)	k_{NO}/k_{NH}[h]
P10	Air	410		4.59×10^6	0.22	2.09×10^9	
	N_2	410		3.27×10^6	30.6		
	Q1/N_2	410		5.19×10^4		1.5×10^9	
P11	Air	410		4.00×10^6	0.25	1.82×10^9	
	N_2	410		2.54×10^4	39.4		
	Q1/N_2	410		4.68×10^4		2.14×10^9	
P12	Air	410		4.71×10^6	0.21		2.02
	N_2	410		4.98×10^4	20.1		
P13	Air	410	M	4.62×10^6	0.21	2.1×10^9	
	N_2	410	M	6.69×10^4	0.41		
			B	1.71×10^5 (62%)	19.7		
				3.12×10^4 (38%)			
	Q1/N_2	410	M	7.54×10^4		0.85×10^7	
			B	1.83×10^5 (64%)			
				3.73×10^4 (36%)			
P14	Air	410	M	4.50×10^6	0.22	2.05×10^9	
	N_2	410	M	5.64×10^4	17.7		
			B	1.51×10^5 (63%)			
				2.63×10^4 (37%)			
	Q1/N_2	410	M	6.57×10^4		0.93×10^7	
			B	1.68×10^5 (63%)			
				5.32×10^4 (37%)			
P15	Air	410	M	4.68×10^6	0.21	2.1×10^9	
	N_2	410	M	7.25×10^4	13.7		1.29
			B	2.01×10^5 (62%)			1.33
				3.89×10^4 (38%)			1.48

[a] Structure of the probes according to Scheme 1.
[b] Experimental conditions: air-aerated solution: methanol (O_2) = 2.2×10^{-3} mol dm^{-3}; N2 bubbling with stream of nitrogen for 10 min, Q1 = 10^{-3} mol dm^{-3} (1-oxo-2,2,6,6-tetramethyl-4-hydroxypiperidine).
[c] Monitoring wavelength.
[d] Fitting to monoexponential, M or biexponential, B.
[e] Rate constant of decay.
[f] Life-time of the excited state.
[g] Bimolecular rate constant of quenching by oxygen and Q1.
[h] Ratio of the rate constant of the oxidised and parent probe.

4. Conclusions

The triplet route of deactivation of bifunctional probes, where chromophores (naphthalene, 1,8-naphthaleneimide and pyrene) are linked to sterically hindered amine, seems to be a feasible way of electronic energy dissipation. It was clearly demonstrated that triplet state is formed and efficiently quenched by oxygen and *N*-oxyl type of quencher. This quenching with *N*-oxyl is equally efficient as with O_2 for naphthalene and 1,8-naphthaleneimide but less efficient for pyrene. Similarly, the most effective intramolecular quenching is observed for probes where naphthalene was linked with *N*-oxyl and the least effective is for bonded pyrene.

The conclusions concerning the mechanism involved in intermolecular as well as intramolecular quenching are not straightforward. The energy of the states taking part in the system is well defined on the part of donors. The singlet and triplet levels are 385, 255 kJ mol^{-1} [26] for naphthalene, 331, 221 kJ mol^{-1} [27] for 1,8-naphthaleneimide and for pyrene 323 and 210 kJ mol^{-1}, respectively. The energy of the singlet and triplet levels of sterically hindered *N*-oxyls has not yet been determined. Since the singlet state of these donors is efficiently quenched by *N*-oxyls, its singlet level lies probably below 320 kJ mol^{-1}. The inefficient intermolecular and intramolecular quenching of pyrene triplet by *N*-oxyls indicates that triplet levels of donor and acceptor are quite similar when electronic energy transfer is involved.

On the other hand, there might be an involvement of electron transfer for pairs with 1,8-naphthaleneimide as donor [15]. Recently, it has been determined that the rate for electron transfer from nucleotides to excited state of *N*-(3-propanol)-1,8-naphthaleneimide occurred with rate of 2×10^7 for guanidine 5′-monophosphate but with other base phosphates two orders of magnitude slower [27]. Strong solvent effect in the intramolecular quenching of N13 supports involvement of electron transfer as well.

In conclusion the photophysical processes seem to be more important for deactivations linked pairs naphthalene or pyrene with *N*-oxyl. However, the chemical process namely electron transfer is more important for 1,8-naphthaleneimide as donor.

Acknowledgements

The authors thank NATO for support through collaborative research grant OUTR.CRG 961074 for support of laser flash photolysis measurements and projects of Grant agency VEGA 2/4005/97 and 2/7009/20 supporting the work of synthesis and characterisation of probes.

References

[1] J.R. White, A. Turnbull, J. Mater. Sci. 29 (1994) 584.
[2] J. Pospíšil, Adv. Polym. Sci. 124 (1995) 89.
[3] E.N. Step, N.J. Turro, P.P. Klemchuk, M.E. Gande, Angew. Makromol. Chem. 232 (1995) 65.
[4] I. Rossi, A. Venturini, A. Zedda, J. Am. Chem. Soc. 121 (1999) 7914.
[5] A.R. Watkins, Chem. Phys. Lett. 29 (1974) 526.
[6] A.R. Watkins, Chem. Phys. Lett. 70 (1980) 230.
[7] A.R. Watkins, Chem. Phys. Lett. 70 (1980) 262.
[8] J.C. Scaiano, Chem. Phys. Lett. 79 (1981) 41.
[9] V.A. Kuzmin, A.S. Tatikolov, Chem. Phys. Lett. 51 (1977) 45.
[10] J.A. Green II, I.A. Singer, J. Am. Chem. Soc. 96 (1974) 2730.
[11] S.K. Chattopadhyay, P.K. Das, G.L. Hug, J. Am. Chem. Soc. 105 (1983) 6205.
[12] J. Karpiuk, Z. R Grabowski, Chem. Phys. Lett. 160 (1989) 451.
[13] P. Hrdlovič, J.C. Scaiano, I. Lukáč, J.E. Guillet, Macromolecules 19 (1986) 1637.
[14] S. A Green, D. J Simpson, G. Zhou, P.S. Ho, N. V Blough, J. Am. Chem. Soc. 112 (1990) 7337.
[15] S. Green, M.A. Fox, J. Phys. Chem. 99 (1995) 14752.
[16] S. Jockusch, G. Dedola, G. Lem, N.J. Turro, J. Phys. Chem. B 103 (1999) 9126.
[17] J.C. Scaiano, T.J. Connoly, N. Mohtat, C.N. Pliva, Can. J. Chem. 75 (1996) 92.
[18] P. Hrdlovič, Š. Chmela, L. Bučsiova, Chem. Papers 50 (1996) 271.
[19] P. Hrdlovič, Š. Chmela, M. Danko, J. Photochem. Photobiol. A: Chem. 112 (1998) 197.
[20] Š. Chmela, M. Danko, P. Hrdlovič, Polym. Degrad. Stab. 63 (1999) 159.
[21] P. Hrdlovič, Š. Chmela, L. Horinová, Can. J. Chem. 73 (1995) 1948.
[22] P. Hrdlovič, Š. Chmela, J. Photochem. Photobiol. A: Chem. 105 (1998) 83.
[23] L. Bucsiová, Š. Chmela, P. Hrdlovič, Polym. Degrad. Stab., in press.
[24] Š. Chmela, P. Hrdlovič, Chem. Papers 38 (1984) 199.
[25] P. Mezellier, M. Sarakha, A. Rossi, M. Bolte, J. Photochem. Photobiol. A: Chem. 115 (1998) 117.
[26] S.L. Murov, I. Carmicheal, L.G. Hug, Handbook of Photochemistry, 2nd Edition, Marcel Dekker, New York, 1993.
[27] J.E. Rodgers, L.A. Kelly, J. Am. Chem. Soc. 121 (1999) 3854.